铝合金变极性等离子弧穿孔焊过程控制

韩永全[1], 杜茂华[1], 陈树君[2], 吴永军[1], 石 岩[1]
(1. 内蒙古工业大学 材料学院, 呼和浩特 010051;
2. 北京工业大学 机械与应用电子学院, 北京 100124)


韩永全

摘 要: 分析了铝合金变极性等离子弧穿孔立焊工艺特点, 提出了通过对焊接参数的精确控制, 实现变断面铝合金变极性等离子弧穿孔立焊工艺的方法, 并将焊接电流、离子气流量和焊接速度确定为变断面铝合金变极性等离子弧穿孔立焊过程的被调节参数. 保持穿孔熔池上"热"和"力"的动态平衡是调节焊接参数的根本依据, 是实现变断面试件自动焊接的关键所在. 采用单片机为核心的控制器对焊接参数进行实时调节, 动态保持穿孔熔池上热和力平衡, 实现了变断面铝合金变极性等离子弧穿孔立焊工艺.

关键词: 变极性等离子弧焊接; 变断面; 控制
中图分类号: TG456.2 文献标识码: A 文章编号: 0253-360X(2010)11-0093-04

0 序 言

铝合金具有重量轻、比强度高和耐腐蚀性好等特点, 因此, 在重要焊接结构中的应用越来越广. 变极性等离子弧 (简称 VPPA)焊接方法具有能量集中、电弧挺度大、焊后变形小等优点[1,2], 在航空航天重要铝合金结构的焊接中具有良好的应用前景. 变断面铝合金变极性等离子弧穿孔立焊工艺研究是一项新的课题. 目前国内对变断面铝合金变极性等离子弧穿孔立焊工艺研究仍属空白, 并对铝合金变极性等离子电弧形态及特性的研究不够系统, 对该焊接工艺本质的了解还不够全面. 在大型阶梯形铝合金储罐和火箭筒体铝合金焊接结构中存在变断面焊接结构, 只有在掌握铝合金变极性等离子电弧特性及其铝合金变极性等离子穿孔立焊工艺稳定性的基础上, 对多个焊接参数的实时联合精确控制才能实现变断面铝合金变极性等离子弧自动焊接工艺[1-3]. 作者自行研制开发了微机控制的双逆变 VPPA-2型铝合金变极性等离子弧焊接电源, 建立了以 80C196KC单片机为核心的变极性等离子弧穿孔立焊控制系统. 在原有铝合金等离子穿孔焊接工艺研究基础上, 通过对焊接电流、离子气流量和焊接速度的实时联合控制, 国内首次实现了变断面铝合金变极性等离子弧自动焊接工艺.

收稿日期: 2009-07-20
基金项目: 国家自然科学基金资助项目(50764007); 国家自然科学基金资助项目(50775003)

1 试验方法

试验采用了自行研制的变极性等离子焊接电源. 焊接主电源是以 80C196KC单片机为控制核心, 主电路为双逆变型电路拓扑结构. 电源正、反极性最大输出电流可达 400 A, 正极性时间的调节范围为 1~999 ms, 反极性时间的调节范围为 1~99 ms. 单片机通过对离子气流量控制器和步进电机驱动器的控制, 对离子气流量和焊接速度进行精确控制. 采用 YB005-01型压力变送器测试变极性等离子电弧压力, 采用汉诺威分析仪测试电流电压. 试验材料采用了 6~12 mm厚度均匀变化的 ID10(Al-Cu-Mg-Si)铝合金.

2 控制方法的选择

焊接过程中由于试板断面始终变化, 致使图像检测传感小孔的方法很难用于该焊接方法的实时控制. 因为不同断面处最理想的小孔尺寸不同, 所以在未知试板断面厚度情况下, 实时检测到的小孔尺寸并不能反映此时焊接过程是否处于最佳状态.

在变断面铝合金变极性等离子弧焊接过程中, 通过实时调节焊接电流、离子气流量等重要参数, 改变等离子电弧功率和电弧压力大小及其分布, 以此保持变断面铝合金穿孔熔池的稳定存在, 这是实现变断面铝合金变极性等离子弧焊接工艺的关键[3]. 随铝合金试件厚度变化, 保持穿孔熔池稳定存在所

需的等离子电弧功率和电弧压力均发生变化，只有保持穿孔熔池上“热”和“力”的平衡要求，才能实现变断面试件等离子弧穿孔焊接工艺．因此，保持穿孔熔池上“热”和“力”的平衡条件成为了焊接参数的调节依据．文中采取了对焊接参数的实时调节，改变变极性变等离子电弧能量和电弧压力，实时保持穿孔熔池所需能量与变极性等离子弧提供的能量相平衡的控制策略．

3 变断面铝合金等离子弧焊接控制

根据变断面铝合金等离子弧自动焊控制策略，需经大量不同厚度试件焊接试验，获得试板厚度与电弧压力和电弧能量的对应关系，才能为焊接参数的自动调节提供依据．图 1和图 2分别为在不同厚度平板焊接试验过程中采用 YB005—01型压力变送器和汉诺威分析仪测试并计算得到的等离子电弧压力和电弧功率的变化区间图．

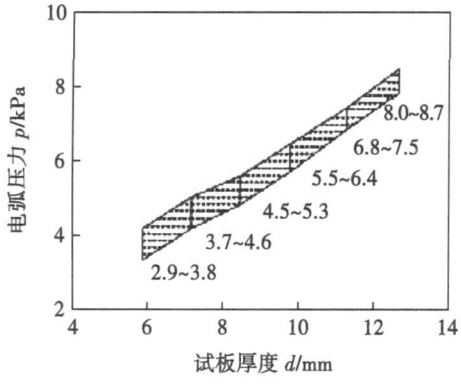

图 1 VPPA 电弧压力变化区间

Fig. 1 Variable curves of VPPA force

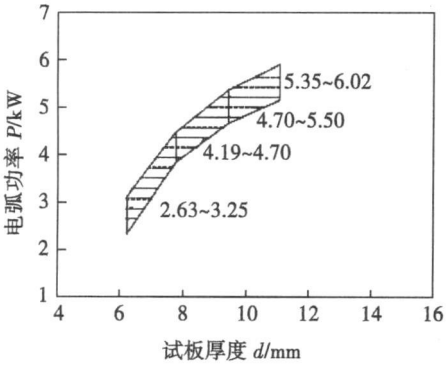

图 2 VPPA 电弧功率变化区间

Fig. 2 Variable curves of VPPA power

从变极性等离子电弧压力和电弧功率变化区间图可看出，随试板厚度的变化所需热和力基本与试板厚度的变化成比例关系．试板厚度超过 10 mm后电弧功率的变化幅度略有减小．分析认为，在外围散热条件不变的情况下，当试板厚度达到一定值后散热趋于稳定值．因此熔化所需热能的增大幅度小于试板厚度增加的幅度．

3.1 控制参数的选定

变断面铝合金变极性等离子弧焊工艺的实现关键在于焊接系统的硬件和软件部分是否具备焊接变断面试件的调节功能．如焊接电源的输出功率必须能够达到变断面试件最大厚度处所需功率值；根据试板断面尺寸变化，焊接电源可独立调节正、反极性电流初始值、终值和变化斜率；离子气流量可以按试板尺寸和穿孔焊接工艺要求，方便地设定起始值、终值和变化斜率．

在铝合金变极性等离子弧焊接工艺中可调参数很多，但有些参数在焊接之前一经确定，焊接过程中就无法更改，如喷嘴和电极参数等．因此，变断面试板焊接时，只能通过焊接过程中可调参数的调节来达到最佳焊接效果．铝合金变极性等离子弧焊接过程中可调参数包括焊接电流（平均电流，正极性电流，反极性电流），正、反极性时间，离子气流量，焊接速度，焊枪高度和送丝速度等．

根据铝合金变极性等离子弧焊接工艺特点确定了焊接电流、离子气流量和焊接速度作为变断面铝合金变极性离子弧焊接过程实时调节参数．图 3为焊接过程自动控制原理框图．

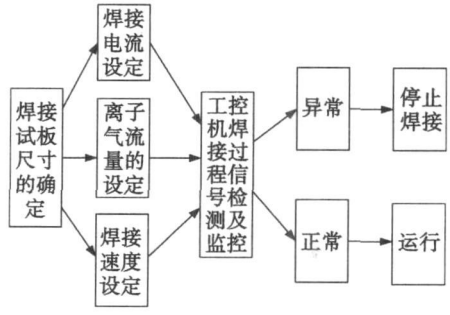

图 3 VPPA焊接过程自动控制原理框图

Fig. 3 Schematic of automatic control VPPAW process

研究认为在铝合金变极性等离子弧焊接中正极性电流对等离子电弧压力影响大，而反极性电流对等离子电弧热影响大．试板厚度不同时对等离子电弧“力”和“热”具有不同的需求[4]．焊接初始段，需较大幅度调节正极性电流幅值来补充电弧压力．此段清理氧化膜的变化量不大，因此要求反极性电流变化幅度不易过大．随着变断面试件焊接过程的进行，电弧压力和氧化膜清理变化需求也随之发生变

化，因此必须根据试板厚度变化，调整焊接参数的调整策略．图 4为焊接电流递升程序．

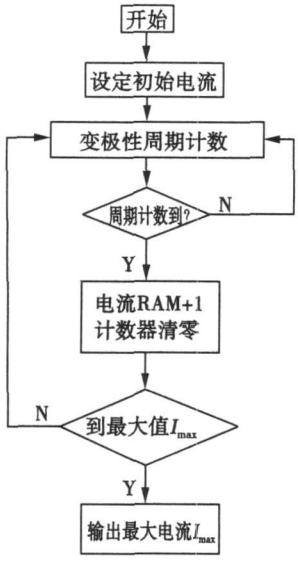

图 4　焊接电流递升程序

Fig. 4　Program of welding current

离子气流量的变化不仅影响电弧压力，而且改变变极性等离子电弧电压[5]．电弧电压的改变，表明电弧功率的变化，电弧功率变化必然影响变极性等离子电弧对穿孔熔池上的热输入．因此，当进行变断面铝合金变极性等离子弧穿孔立焊时，改变离子气流量要同时考虑电弧压力和电弧能量的变化量，否则无法满足穿孔熔池上“力”和“热”的平衡状态，也就不能实现变断面铝合金变极性等离子弧穿孔 立焊．图 5为离子气流量调节程序．工件行走机

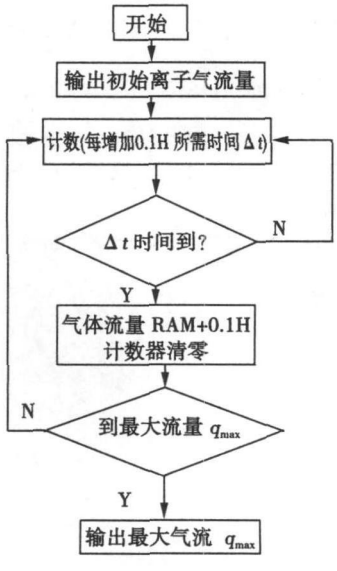

图 5　离子气流量调节程序

Fig. 5　Regulate program of plasma gas flux

构由单片机控制系统、步进电机、步进电机驱动器和滑架等组成．单片机发出的调节焊接速度指令通过步进电机驱动器改变电机转速，调整工件行走速度．

3.2　变断面铝合金等离子弧焊接工艺试验

喷嘴结构、钨极尺寸、钨极内缩量等参数在正常焊接情况下，对不同厚度试板所选择的喷嘴容量、孔径和内缩量应该不同．研究中发现，采用较大孔径喷嘴、大直径钨极时，通过调节离子气流量、焊接电流等参数可进行薄板铝合金焊接，但采用小喷嘴孔径、小钨极直径时，则很难通过调节其它焊接工艺参数进行厚板铝合金穿孔焊接．原因在于采用小孔径喷嘴条件下，等离子电弧形态及温度分布很难得到厚板铝合金穿孔熔池上合适的温度梯度和受力状态，并且调节不当，易出现“双弧”等现象．

表 1为通过大量试验获得的 6～12 mm变断面铝合金变极性等离子弧焊接最佳焊接工艺参数．

表 1　焊接工艺参数

Table 1　Welding parameters

试板厚度 d/mm	离子气流量 q_v/(L·min^{-1})	EN极性电流 I_N/A	EP极性电流 I_P/A	焊接速度 v/(mm·min^{-1})
6～12	2～3	130	185	15～20

图 6为 6～12 mm变断面铝合金实际穿孔焊接过程中采用汉诺威分析仪测到电流、电压值，再经计算获得的电弧功率变化曲线．从实际焊接电弧功率曲线看，变极性等离子电弧功率变化在图 2区间之内，说明焊接过程中穿孔熔池上热达到了平衡．

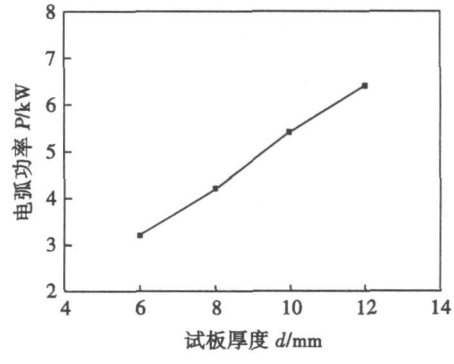

图 6　电弧功率变化曲线

Fig. 6　Variable curves of arc power

图 7为 6～12 mm变断面铝合金实际穿孔焊接过程中采用 YB005—01型压力变送器测到的等离子电弧压力变化曲线．电弧压力曲线变化基本在图 1区间范围之内．说明通过程序控制实现穿孔熔

池上所需力的平衡.

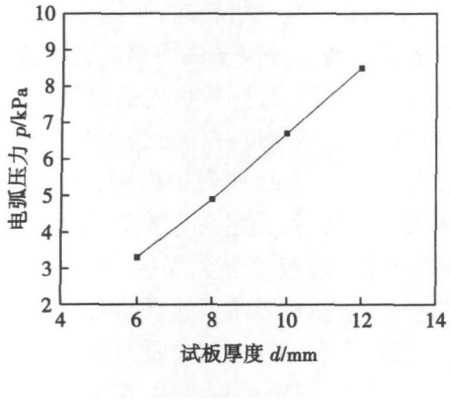

图 7 电弧压力变化曲线

Fig. 7 Variable curves of arc force

图 8为 6~12 mm变断面铝合金焊缝形貌. 从图上可以看出正、反面成形良好, 余高均匀.

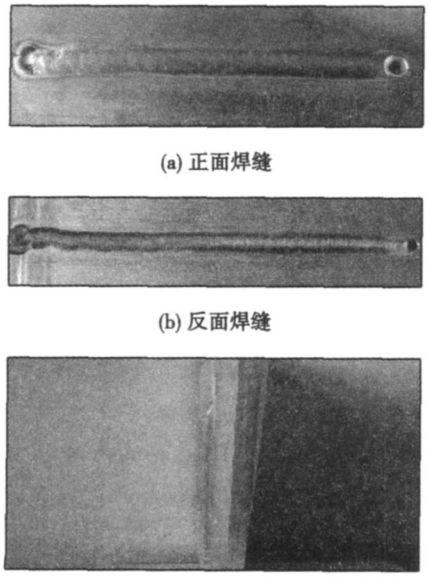

图 8 6~12 mm变断面铝合金 VPPA焊缝

Fig. 8 Weld of 6~12 mm variable cross-section

试验结果证实了铝合金变极性等离子弧自动焊接系统的控制精度高, 选择的控制参数合理. 满足了变断面铝合金变极性等离子弧穿孔熔池稳定性要求.

4 结 论

(1) 提出了通过对焊接参数的程序控制, 实现变断面铝合金变极性等离子弧穿孔立焊工艺的方法, 并将焊接电流、离子气流量和焊接速度确定变断面铝合金焊接过程中的调节参数. 以 80C196KC单片机作为控制核心, 完成了能够精确控制焊接电流、离子气流量和焊接速度的变极性等离子弧立焊控制系统.

(2) 变极性等离子弧焊接平均电流为 142~225 A, 离子气流量为 2~3 L/min, 焊接速度为 15~20 mm/min变化时能够保持 6~12 mm变断面铝合金变极性等离子弧穿孔焊接熔池上热和力平衡, 获得良好的焊缝.

参考文献:

[1] Nunes, Bayless E O. Variable polarity plasma arc welding on space shuttle external tank[J]. Welding Journal, 1984, 63(4): 27-35.

[2] Artinez L F, Matlock C, Marques R F, et al. Effect of weld gases on melt zone size in VPPA welding of A l2219[J]. Welding Journal, 1994, 73(10): 51-55.

[3] 美国焊接学会. 焊接新技术[M]. 韩鸿硕, 张 桂, 译. 北京: 宇航出版社, 1987.

[4] 韩永全, 陈树君, 殷树言, 等. 大厚度铝合金变极性等离子弧穿孔立焊技术[J]. 机械工程学报, 2006, 42(9): 144-148.
Han Yongquan, Chen Shujun, Yin Shuyan, et al. Variable polarity plasma arc welding process for thick aluminum alloy[J]. Chinese Journal of Mechanical Engineering, 2006, 42(9): 144-148.

[5] 安藤弘平. 焊接电弧现象[M]. 施雨湘, 译. 北京: 机械工业出社, 1985.

作者简介: 韩永全, 男, 1971年出生, 博士, 教授. 主要研究方向为新型焊接设备及焊接过程控制. 发表论文 20余篇.

Email: mmhyq@sina.com

proved that carbide rupture caused crater-like pits.

Key words: Fe-Cr-C hardfacing alloy; abrasive wear mechanism; carbide; desquamation

Susceptibility to intergranular corrosion of Super 304H stainless steel welded joint / LI Xinmei, ZOU Yong, ZHANG Zhongwen, ZOU Zengda (1. Key Laboratory of Liquid Structure and Heredity of Materials, Ministry of Education, Shandong University, Jinan 250061, China; 2. Shandong Electric Power Research Institute, Jinan 250002, China). p. 77—80

Abstract: The susceptibility to intergranular corrosion for weld and base metal of Super 304H steel was investigated by double loop electrochemical potentiodynamic (EPR). The experimental results indicate that the weld and base metal have the lower tendency of intergranaular corrosion. The microstructure of weld and base metal was investigated by means of scanning electron microscopy, electron probe micro-analysis, X-ray diffraction and transmission electron microscope. The results showed that both the weld and the base metal were consisted of γ-matrix and some precipitated phase, no obvious $Cr_{23}C_6$ was detected. Therefore, no chromium depleted zone was formed. However, the susceptibility to intergranular corrosion of weld is better than that of base metal due to the difference of alloy elements.

Key words: Super 304H steel; electrochemical potentiokinetic reactivation; welded joint; intergranular corrosion

Extraction of weak signal for weld defect and its qualification in joint interface between dissimilar materials / GAO Shuangsheng, CHI Dazhao, GANG Tie (1. School of Materials Science & Engineering, Shenyang Aerospace University, Shenyang 110036, China; 2. State Key Laboratory of Advanced Welding Production Technology, Harbin Institute of Technology, Harbin 150001, China). p. 81—84

Abstract: By employing pre-processing of morphologic enhancement and area-reconstruction, a novel method for image segmentation was presented based on watershed transformation. And using the method, ultrasonic test image for a joint interface between dissimilar materials was segmented. To validate the reliability of this method, the sample was destructed and tested. The results show that over-segmentation caused by traditional watershed transformation can be avoided by pre-procession of morphologic enhancement and area-reconstruction. Meanwhile, the test image can be blocked adaptively according to the distribution feature of defect and then the defect can be extracted and quantified by threshold segmentation. Destructive experiment shows the presented method is very efficient with high reliability.

Key words: joint between dissimilar materials; C-scan image; defect with weak signal; watershed transformation; area-reconstruction

Nonlinear multiple regression modeling of nugget formation for dissimilar steel welding with unequal thickness / LUO Yi, LI Chuntian, ZHOU Yin (1. School of Materials Science and Engineering, Chongqing University of Technology, Chongqing 400050, China; 2. School of Business Management, Chongqing 401147, China). p. 85—88

Abstract: In order to investigate the resistance spot welding process for dissimilar steel sheet with unequal thickness, nonlinear multiple orthogonal regression assembling was applied to design the experiment. By taking nugget diameter and nugget deviation of spot welds as the study indexes and welding parameters such as welding current, electrode force, welding current duration and heat treatment pulse current, and interactions among them as the influencing factor, a nonlinear multiple regression model of nugget geometry parameters was developed. The results showed that there was an effective prediction on nugget size by the optimized models. With these prediction results, the welding process was also optimized based on the analysis on the effects of parameters and their interactions on the welding quality.

Key words: resistance spot welding; unequal-thickness materials; nugget geometry; welding process; regression model

Regression analysis on maximum vibratory welding temperature at different parameters / LIU Qinghua, XU Jijia, CHEN Ligong, YU Zhishui (1. School of Materials Engineering, Shanghai University of Engineering Science, Shanghai 201620, China; 2. School of Materials Science and Engineering, Shanghai Jiao Tong University, Shanghai 200240, China). p. 89—92

Abstract: Plate butt welding tests at different vibratory welding parameters were designed to investigate the influence of welding heat input and vibratory acceleration on maximum welding temperature. A mathematic model of maximum temperature was founded based on the multivariant nonlinear regression analysis. The results show that the peak temperature increases with the increase of vibratory acceleration at the higher welding heat input. The peak temperature increases initially and then decreases with the increase of vibratory acceleration at medium and lower welding heat input. According to the test results of correlation, linear regression significance and regression coefficients significance, the proposed model is feasible. The relationship between the regression coefficient related to vibratory acceleration and the distance of measuring points to weld center line was studied. The results show that vibratory acceleration has a significant effect on the temperature of the molten pool center.

Key words: vibratory welding; maximum temperature; regression analysis

Process control of variable polarity keyhole plasma arc welding for aluminum alloy / HAN Yongquan, DU Miaohua, CHEN Shujun, WU Yongjun, SHI Yan (1. School of Materials Science and Engineering, Inner Mongolia University of Technology, Hohhot 010051, China; 2. School of Mechanical Engineering and Applied Electronics Technology, Beijing University of Technology, Beijing 100124, China). p. 93—96

Abstract: The variable polarity keyhole plasma arc vertical welding process characters of aluminum alloy were analyzed and the method was found that the variable cross-section aluminum alloy was welded with the variable polarity keyhole plasma arc vertical welding by precisely controlling welding parameters. Welding current, the flux of plasma gas and welding speed were defined as the adjusted parameters. The dynamic balance of ther-

mal and force in keyhole weld pool is the key to regulate the welding parameters and realize the automatic welding of variable cross-section sample. The control device of the VPPA welding system was constructed based on 80C196KC. So it can regulate welding parameters in real-time and keep the balance between thermal and force dynamically and realize the variable polarity keyhole plasma arc vertical welding process of variable cross-section aluminum alloy.

Key words: variable polarity plasma arc; variable cross-section; control

Brazing process of alumina ceramic to steel ZHANG Wanhong[2], LI Ning[1] (1. School of Materials Science & Engineering, Henan University of Science and Technology, Luoyang 471003, Henan, China; 2. Henan Key Laboratory of Advanced Non-ferrous Metals, Luoyang 471003, Henan, China). p 97—100

Abstract: Ceramics/metals joining is widely applied in aerospace and electronic industry instruments, fuel cells fields. Al_2O_3 ceramic was brazed to Q235 steel in vacuum with active filler alloys Cu75Ti25, Cu70Ti30, Cu80Ti20 and Cu85Ti15, respectively. The bending strength of each specimen and the microhardness of the interface were tested, and the results showed that the Cu75Ti25 filler was the best ratio of filler metal, and the optimum brazing parameters were 1 100 ℃ and 20 minutes. At the optimized temperature, the active filler alloy melts sufficiently and fills joint gap, then mutually diffuse into ceramic and steel sides. The bonding interface is composed of three layers of reaction layer formed by microporous ceramics filled with liquid active alloy, Ti-Cu alloy layer and steel side diffused layer. XRD analysis shows that AlCu, Cu_3TiO_4, TiC, $TiFe_2$ phases form in the bonding zone, and the microstructure of bonding area is dense and there are no defects. Accordingly a good metallurgical combination of ceramic/steel is achieved.

Key words: active brazing; Cu75Ti25; Al_2O_3 ceramics; Q235 steel; interface

Influence of boundary condition on high frequency inducting plate bending ZHOU Hong[2], LI Gan[2], ZHU Hongjuan[1] (1. School of Naval Architecture and Ocean Engineering, Jiangsu University of Science and Technology, Zhenjiang 212003, Jiangsu, China; 2. School of Naval Architecture, Ocean and Civil Engineering, Shanghai Jiao Tong University, Shanghai 200030, China). p 101—104

Abstract: The plate bending process by high frequency induction heating apparatus was analyzed with ANSYS software based on the thermal-elastic-plastic finite element analysis for the mild steel plate. Numerical results were used to qualitatively analyze the influences of the changes of material and panel boundary condition on the temperature field, final shrinkage and angular distortion, which can provide the digital support for automatic machining of ship plates. The results showed that the total stress in plate would increase, low-stress zone would decrease and the transverse shrinkage would increase when the constraint points increased at the edges of the longitude direction. At the same time, the longitudinal shrinkage and the transverse angular distortion are opposite to the transverse shrinkage trend. But the longitudinal angular distortion decreases firstly and then increases with the increase of constraint points at the edges of the longitude direction. With the constraint being strengthened, the displacements at different directions decrease.

Key words: high-frequency induction heating; curved plate bending; residual plastic strain; thermal-elastic-plastic finite element

Reconstruction of emission coefficients for welding arc based on iterative algorithm XIONG Jun, ZHANG Guangjun, HU Yutang (State Key Laboratory of Advanced Welding Production Technology, Harbin Institute of Technology, Harbin 150001, China). p 105—108

Abstract: This investigation attempted to retrieve the emission coefficients of welding arc by an algebraic reconstruction technique (ART). The ART algorithm was programmed with MATLAB language, and a displaced Gaussian model was used to validate the efficiency of the program. The intensities of a free burning arc were acquired by the imaging method. The emission coefficients were reconstructed by the developed ART program, and the results were compared to that reconstructed by the extensively used Abel inversion. The results show that the ART algorithm has a high precision and can be used for the reconstruction of emission coefficients of welding arc.

Key words: welding arc; spectroscopic diagnosis; emission coefficient; ART algorithm

Analysis on electrode displacement fluctuation characteristics in AC resistance spot welding WANG Xianfeng, MENG Guoxiang, XIE Wenhua, FENG Zhengjin (School of Mechanical and Power Engineering, Shanghai Jiao Tong University, Shanghai 200240, China). p 109—112

Abstract: The signals of electrode displacement and welding current were sampled by the improved monitoring system of AC resistance spot welding (RSW). The fluctuation characteristics of the electrode displacement were analyzed, and it was concluded that the displacement fluctuation was caused by 50 Hz AC resistance heat pulse. The mechanism of electrode displacement fluctuation was analyzed by onion phenomenon in RSW, and the results showed that the electrode displacement was mainly caused by thermal expansion before the nugget formation and by phase transition expansion after that, and there were the fluctuation characteristics in both expansion. The power factor angle, dynamic resistance and dynamic resistance heat were calculated with the firing angle and conduction angle provided by the welding current curve. Through the comparative analysis on the peak of the displacement fluctuation cycle and the dynamic resistance heat, it was found that the former was sensitive to the thermal and phase transition expansion, and can be used to reflect the different stages of the nugget formation process.

Key words: resistance spot welding; electrode displacement; fluctuation characteristics; thermal expansion; phase transition expansion